CUMULATIVE SUM CHARTS FOR HIGH YIELD PROCESSES

T. C. Chang and F. F. Gan

Infineon Technologies Melaka and National University of Singapore

Abstract: The cumulative sum (CUSUM) chart, well-known to be sensitive in detecting small and moderate parameter changes, is proposed here for monitoring a high yield process. The sensitivities of the CUSUM charts based on geometric, Bernoulli and binomial counts are compared. Based on the comparisons, recommendations for the selection of a chart are provided. Simple procedures are given for optimal design of CUSUM charts based on geometric and Bernoulli counts. An application of CUSUM charts in monitoring an actual high yield process is demonstrated.

Key words and phrases: Bernoulli counts, geometric counts, Markov chain, parts-per-million, statistical process control.

1. Introduction

In the manufacturing industry, many processes are producing very low levels of nonconforming items due to the advent of technological advancement and manufacturing automation. The fraction p of nonconforming items for such processes is usually on the order of parts-per-million (ppm) and one speaks of high yield processes. A high yield process is defined here as a process with an in-control p_0 of at most 0.001, or 1000 ppm. The Shewhart np or p chart, commonly used for monitoring the fraction of nonconforming items, is not suitable for monitoring high yield processes. Goh (1987) showed that use of this chart results in high false alarm rates and inability to detect process improvements. In the quality control literature, most charts for monitoring high yield processes are based on a geometric count, the count of items inspected until a nonconforming item is found.

Indeed, most are based on transformed geometric counts. Calvin (1987) was the first to propose the Shewhart chart based on geometric counts; Nelson (1994) proposed a Shewhart chart based on $X^{\frac{1}{3.6}}$ where X is a geometric count; Quesenberry (1995) proposed several charts based on $Q = -\Phi^{-1}\{1 - (1 - p_0)^X\}$, $\Phi^{-1}(\cdot)$ the inverse distribution function of the standard normal random variable; McCool and Motley (1998) considered Shewhart and exponentially weighted moving average (EWMA) charts based on $Y = X^{\frac{1}{3.6}}$ and $Z = \ln(X)$. The main argument for using a transformation of geometric counts is to obtain an approximate

normal distribution. Shewhart, CUSUM and EWMA charts which have been developed for normally distributed data can then be used.

The main disadvantage in implementing a chart based on transformed measurements is the difficulty in interpretation. In addition, some transformations involve complicated calculations not easily done without the use of a computer. Design procedures for CUSUM charts based on nontransformed geometric counts have not been developed. Even though Bourke (1991) has given a design procedure for the geometric CUSUM charts, it is only meant for an in-control p_0 of at least 0.002. Bourke (1991) noted that for very small in-control p_0, the use of the Markov chain approach in determining average run length (ARL) results in a very large matrix for inversion and is computationally prohibitive.

Reynold and Stoumbos (1999) proposed the monitoring of p using a Bernoulli CUSUM chart, using the corrected diffusion (CD) approach for approximating the average number of items sampled (ANIS) until a signal is issued. The CD approach is found to work well for $p > 0.01$. However, the accuracy of the CD approach for $p < 0.01$ has not been evaluated. They provided a procedure for designing an upper-sided Bernoulli CUSUM chart for an in-control $p_0 > 0.001$. A comparison of the run length performances given by Reynold and Stoumbos (1999) showed that the Bernoulli CUSUM chart is more sensitive in detecting increases in p than the Shewhart and CUSUM charts based on binomial counts for an in-control p_0 of 0.01. They also noted, without proof, that an upper-sided CUSUM chart with head start based on Bernoulli counts is equivalent to an upper-sided CUSUM chart based on geometric counts without head start.

The main objective of this paper is to provide procedures for designing optimal CUSUM charts for monitoring a high yield process. CUSUM charts based on nontransformed geometric and Bernoulli counts are developed. Explicit formulae for determining the exact ANIS of both the upper- and lower-sided Bernoulli CUSUM charts are given. These formulae are based on the Markov chain approach. The accuracy of the CD approach for calculating the ANIS for p less than 0.01 is evaluated for both the upper- and lower-sided charts. The conditions for an upper-sided Bernoulli CUSUM chart to be equivalent to an upper-sided geometric CUSUM chart is also given. The run length performances of CUSUM charts based on geometric, Bernoulli and binomial counts in detecting both increases and decreases in p are evaluated. Based on our comparisons, recommendations for the selection of a chart are provided. Optimal design procedures for the CUSUM charts are also given. An application of the CUSUM charts in monitoring the fraction of nonconforming items of a specific high yield process is demonstrated.

2. The CUSUM Charts

2.1. CUSUM charts based on Bernoulli and binomial counts

The CUSUM chart is more sensitive to small and moderate parameter changes than the Shewhart chart. The CUSUM chart is also known to be comparable to the EWMA chart in terms of run length performance for many processes. The traditional approach of monitoring p involves taking samples at regular intervals with the binomial count of nonconforming items taken to be the measurement of quality. A large binomial count indicates a possible deterioration in quality and, on the other hand, a small count indicates a possible improvement in quality. The upper-sided CUSUM chart for detecting an increase in p plots $S_t = \max\{0, S_{t-1} + X_t - k_S\}$ against t for $t = 1, 2, ...$, where X_t is the count of nonconforming items obtained for sample number t. Here k_S is a constant and the starting value $S_0 = u$, $0 \leq u < h_S$. A signal is issued at the first t for which $S_t \geq h_S$. Similarly, the lower-sided CUSUM chart for detecting a decrease in p plots $T_t = \min\{0, T_{t-1} + X_t - k_T\}$ against t for $t = 1, 2, ...$, where k_T is a constant and $T_0 = v$, $-h_T < v \leq 0$. A signal is issued at the first t for which $T_t \leq -h_T$. A two-sided CUSUM chart is obtained by running the two one-sided CUSUM charts simultaneously.

The reference values k_S and k_T are obtained from the sequential probability ratio test (SPRT) approach for testing $H_0 : p = p_0$ versus $H_1 : p = p_1$, where p_0 is the in-control p and p_1 is the out-of-control p. Then

$$k = \frac{n \ln\{(1 - p_0)/(1 - p_1)\}}{\ln\{p_1(1 - p_0)/p_0(1 - p_1)\}}.$$

Moustakides (1986) showed that such a choice is optimal in terms of run length performance. Reynold and Stoumbos (1999) suggested that for the Bernoulli CUSUM chart, the reference value k can be approximated to $1/c$ where c is an integer. With this approximation, the head starts and the possible CUSUM's will be integer multiples of $1/c$ and this is convenient for plotting the chart. This approach is adopted here.

2.2. CUSUM charts based on geometric counts

Another approach to the monitoring of p is based on the geometric count, the count of items inspected until a nonconforming item is found: a small count indicates a possible deterioration in quality, a large count indicates a possible improvement in quality. The upper-sided CUSUM chart for detecting an increase in p plots $H_t = \max\{0, H_{t-1} + k_H - Y_t\}$ against t for $t = 1, 2, ...$, where Y_t is the tth geometric count. Here k_H is a constant and the starting value $H_0 = u$, $0 \leq u < h_H$. A signal is issued at the first t for which $H_t \geq h_H$. Similarly, the lower-sided CUSUM chart for detecting decreases in p plots $L_t = \min\{0, L_{t-1} + k_L - Y_t\}$

against t for $t = 1, 2, ...$, where k_L is a constant and $L_0 = v$, $-h_L < v \leq 0$. A signal is issued at the first t for which $L_t \leq -h_L$. A two-sided CUSUM chart is obtained by running the two one-sided CUSUM charts simultaneously. The reference values k_H and k_L are based on the SPRT approach as

$$k = \frac{\ln\{p_1(1 - p_0)/p_0(1 - p_1)\}}{\ln\{(1 - p_0)/(1 - p_1)\}}.$$

Note that for the Bernoulli CUSUM charts, k_S and k_T are the inverse of k_H and k_L of the geometric CUSUM charts, respectively.

The upper-sided Bernoulli CUSUM chart with parameters $k_S = 1/c$, $h_S = h$ and head start $u = (w + c - 1)/c$ is equivalent to the upper-sided geometric CUSUM chart with parameters $k_H = c$, $h_H = ch - c + 1$ and head start $u = w$. (The proof of equivalence can be found in the Appendix.) Then, the ANIS of an upper-sided geometric CUSUM chart can be obtained from the ANIS of the corresponding upper-sided Bernoulli CUSUM chart. For the lower-sided geometric CUSUM chart, a decrease in p will be signalled only when a nonconforming item is detected whereas, for the lower-sided Bernoulli CUSUM chart, a decrease in p will be signalled when sufficient conforming items are detected. Thus, these two charts are not equivalent in detecting a decrease in p.

3. Computation of ANIS of Bernoulli CUSUM Charts

3.1. The exact ANIS of Bernoulli CUSUM chart

The ANIS is used to measure the run length performance of charts. Based on the Markov chain approach, explicit formulae for computing the ANIS of the upper- and the lower-sided Bernoulli CUSUM charts can be obtained. (Details for the upper-sided Bernoulli CUSUM chart are given in the Appendix.) Let $q = 1 - p$. For the upper-sided Bernoulli CUSUM chart with $k_S = 1/c$ and $h_S = (i + c)/c$ where i and c are constants, for $u = 0$,

$$\text{ANIS}_0 = \frac{2\{1 - q^{c-1}(ip + 1)\} + q^{c-i-1}}{p(1 - q^{c-1} - ipq^{c-1})}, \quad \text{for } 0 \leq i \leq c - 1,$$

$$\text{ANIS}_0 = a/b, \quad \text{for } c \leq i \leq 2c - 1,$$

where

$$a = q^{c-1} + 3q^{i-c+1} - 3q^i + pq^{c-1}\{(1+q^{c-1})(c-i-1)+(c-1)\}$$
$$+ \binom{i-c+2}{2}p^2q^{c-2}(q^c - 3q^{i+1}) + 3pq^i\{q^{c-1}(i-c+1)(p(i-c+1)+1)-i\},$$

$$b = p^3 q^{i+c-1} \left\{ (c-i-1)^2 - \binom{i-c+2}{2} \right\}$$
$$+ (c-i-1)p^2 q^i (1-q^{c-1}) + pq^i (q^{1-c} - p(c-1) - 1).$$

For the upper-sided CUSUM with head start $u = (c-1)/c$, $\text{ANIS}_{(c-1)/c} = \text{ANIS}_0 - 1/p$. For the lower-sided Bernoulli CUSUM chart with $k_T = 1/c$ and $h_T = (i+c)/c$, for $v = 0$,

$$\text{ANIS}_0 = \frac{1 + q^c - 2q^{c+i} - ipq^{c-1}}{pq^{c+i}}, \quad \text{for } 0 \leq i \leq c,$$

$$\text{ANIS}_0 = s/t, \quad \text{for } c+1 \leq i \leq 2c,$$

where $t = pq^{c+i}$ and

$$s = 1 - ipq^{c-1} + q^c(q^c - 3q^i + 1) + pq^{2c-2} \left\{ \binom{i-c+2}{2} p + (c-i)q \right\}.$$

These formulae are valid as long as $h_S \leq 3 - 1/c$ and $h_T \leq 3$ are satisfied, common for high yield processes.

3.2. The CD approach for approximating the ANIS

Reynold and Stoumbos (1999) proposed using the corrected diffusion (CD) approach for approximating the ANIS of the Bernoulli CUSUM chart. Siegmund (1979, 1985) originally developed the CD approximation of the ANIS of CUSUM charts by replacing the random walk of the control statistic of a CUSUM chart with a continuous Brownian motion process. The CD approximation works well for the exponential family of continuous distributions. Reynold and Stoumbos (1999) extended the work of Siegmund (1979, 1985) by standardising the Bernoulli random variable and approximating the standardised variable using a Brownian motion process. They showed that for p at least 0.01, the CD approach works well.

Comparisons of the CD approximation with the exact ANIS for p less than 0.01 are performed for both the upper- and lower-sided Bernoulli CUSUM charts. For the upper-sided Bernoulli CUSUM chart with $k_S = 1/69315$, $h_S = 100807/69315$ and $u = 0.0$, the ANIS is 1799 when $p = 0.001$ based on the CD approach, as compared to the exact value of 2000. For the lower-sided Bernoulli CUSUM chart with $k_T = 1/2773$, $h_T = 3230/2773$ and $v = 0.0$, the ANIS is 3729 when $p = 0.00001$ based on the CD approach, as compared to the exact value of 3282. The relative error of the CD approximation can be as large as 13.6%, due mainly to the fact that the Bernoulli distribution with a very small p is highly skewed and the standardised Bernoulli variable is not well approximated by a Brownian

motion process. The CD approximation is thus unsatisfactory for a high yield process.

4. The Run Length Performance of CUSUM Charts

4.1. Upper-sided charts

The ANIS profiles of upper-sided CUSUM charts based on geometric, Bernoulli and Bernoulli binomial counts for monitoring high yield processes are given in Table 1. The geometric Shewhart chart is also included for comparison. All CUSUM charts have an in-control p_0 of 0.0001 and are designed to be optimal in detecting a p value of 0.0003. Due to the discrete nature of the sample statistics, chart parameters are chosen such that the in-control ANIS is as close to 70,000 as possible. Among all charts, the geometric CUSUM chart is found to be more sensitive in detecting increases in p, except for very large ones for which the geometric Shewhart chart is more sensitive. It can be observed from Table 1 that the sensitivity of a binomial CUSUM chart increases as the sample size decreases. Between the CUSUM charts based on Bernoulli and binomial counts, the Bernoulli CUSUM chart is more sensitive. This is due to the fact that the Bernoulli CUSUM chart is able to declare the status of the process after each item is checked.

Table 1. The ANIS profiles of upper-sided geometric Shewhart, geometric CUSUM, Bernoulli CUSUM and binomial CUSUM charts with respect to various p. The in-control p_0 is 0.0001 and the CUSUM charts are optimal in detecting $p_1 = 0.0003$.

	Geometric Shewhart	Geometric CUSUM	Bernoulli CUSUM $n = 1$	Binomial CUSUM $n = 101$	Binomial CUSUM $n = 759$
		$k_H = 5493$	$k_S = \frac{1}{5493}$	$k_S = \frac{1}{54}$	$k_S = \frac{4}{29}$
	$H = 1543$	$h_H = 4662$	$h_S = \frac{9738}{5493}$	$h_S = \frac{95}{54}$	$h_S = \frac{47}{29}$
p		$u = 0$	$u = 0.0$	$u = 0.0$	$u = 0.0$
0.00010	69934.1	69959.2	69732.8	69732.5	69561.2
0.00015	32263.6	29789.4	32947.5	32997.9	33004.2
0.00020	18829.0	16898.6	20157.0	20208.1	20359.3
0.00025	12496.4	11196.7	14128.2	14176.3	14406.8
0.00030	8994.7	*8158.1*	*10743.4*	*10789.2*	*11065.0*
0.00035	6846.1	6329.1	8615.3	8659.8	8963.0
0.00040	5427.5	5129.9	7167.9	7211.5	7532.3
0.00045	4438.4	4292.3	6125.1	6168.4	6500.4
0.00050	3719.1	3678.4	5340.4	5383.6	5723.0
0.00100	1271.6	1445.8	2293.5	2339.0	2682.2
0.00500	200.1	203.1	400.4	450.4	843.9
0.10000	10.0	10.0	20.0	101.0	759.0

4.2. Lower-sided charts

The ANIS profiles of lower-sided CUSUM chart based on geometric, Bernoulli and binomial counts are given in Table 2. The geometric Shewhart chart is also included for comparison. All CUSUM charts have an in-control p_0 of 0.0001 and are designed to be optimal in detecting a p value of 0.00005. Due to the discrete nature of the sample statistics, chart parameters are chosen such that the in-control ANIS is as close to 40,500 as possible. Table 2 reveals that the charts based on geometric counts are not effective in detecting decreases in p, due mainly to the fact that when p decreases the geometric count will tend to be very large. It can be observed from Table 2 that a binomial CUSUM chart based on a larger sample is more sensitive in detecting decreases in p than a binomial CUSUM chart based on a smaller sample.

Table 2. The ANIS profiles of lower-sided geometric Shewhart, geometric CUSUM, Bernoulli CUSUM and binomial CUSUM charts with respect to various p. The in-control $p_0 = 0.0001$ and the CUSUM charts are optimal in detecting $p_1 = 0.00005$.

	Geometric Shewhart	Geometric CUSUM	Bernoulli CUSUM $n = 1$	Binomial CUSUM $n = 100$	Binomial CUSUM $n = 992$
		$k_L = 13862$	$k_T = \frac{1}{13863}$	$k_T = \frac{1}{130}$	$k_T = \frac{1}{14}$
	$h = 13986$	$h_L = 125$	$h_T = \frac{16260}{13863}$	$h_T = \frac{163}{130}$	$h_T = \frac{16}{14}$
p		$v = 0$	$v = 0.0$	$v = 0.0$	$v = 0.0$
0.000100	40498.1	†40468.0	40501.4	40542.8	40515.2
0.000090	39124.2	39159.0	36599.9	36618.7	36538.2
0.000080	38269.5	38288.0	33143.7	33147.8	33017.8
0.000070	38027.7	38018.2	30078.7	30074.6	29898.3
0.000060	38574.7	38529.0	27357.4	27350.4	27130.7
0.000050	40247.6	*40297.2*	*24938.4*	*24932.9*	*24672.6*
0.000040	43742.8	43806.2	22785.7	22785.1	22486.6
0.000030	50711.1	50730.5	20867.6	20874.4	20540.4
0.000020	66138.2	66172.1	19156.2	19172.7	18805.3
0.000010	115011.4	115104.7	17627.5	17655.2	17256.4
0.000005	214486.7	214547.1	16924.8	16958.5	16544.9

† The ANISs of the lower-sided geometric CUSUM charts are simulated such that the standard error of ANIS is less than 0.1% of the ANIS.

4.3. Recommendation of charts for high yield processes

Based on the comparisons of the charts in the previous section, the upper-sided geometric CUSUM chart is recommended for detecting increases in p only.

A decrease in p indicates a possible process improvement. Therefore, if a process engineer is also interested in detecting decreases in p, a two-sided Bernoulli CUSUM chart is recommended. Although the upper-sided geometric and the upper-sided Bernoulli CUSUM charts have the same run length properties (see the Appendix), there is a significant difference between them in terms of implementation. The Bernoulli CUSUM chart plots on every item checked and therefore the "health" of a process is closely monitored, a geometric CUSUM chart is slower to react. On the other hand, a Bernoulli CUSUM chart requires continuous plotting while the geometric CUSUM chart does not.

5. Optimal Design of CUSUM Charts

5.1. The upper-sided geometric CUSUM charts

The following three steps are proposed for the design of an optimal upper-sided geometric CUSUM chart:

Step 1. Determine the in-control p_0 and the out-of-control p_1 for which quick detection is desired.

Step 2. Decide on the in-control ANIS.

Step 3. Based on the information given in Steps 1 and 2, the chart parameters k_H and h_H can be obtained from Table 3.

The in-control p_0 can be estimated using the sample fraction of nonconforming items produced when the process is in-control. The out-of-control p_1 can be taken as the fraction of nonconforming items where a quick detection is needed. The in-control ANIS is often determined by considering the production rate and the costs associated with machine downtime and false alarms.

5.2. The upper- and lower-sided Bernoulli CUSUM charts

The procedure for designing an optimal upper- or lower-sided Bernoulli CUSUM chart is similar to the one for upper-sided geometric CUSUM charts. For Step 3, the chart parameters for an upper- or lower-sided Bernoulli CUSUM chart can be obtained from Table 4 or Table 5 respectively. The parameter k_S or k_T is obtained as $k_S = 1/c$ or $k_T = 1/c$. The two-sided Bernoulli chart can be obtained by running the upper- and lower-sided charts simultaneously. Finally, the ANIS of a two-sided CUSUM chart can be approximated as

$$\text{ANIS}_2 \approx \frac{\text{ANIS}_L \cdot \text{ANIS}_U}{\text{ANIS}_L + \text{ANIS}_U},$$

where ANIS_U and ANIS_L are the ANIS's of the upper- and lower-sided charts respectively. The conditions for the ANIS formula to be exact is similar to that of Lucas (1985).

Table 3. The optimal chart parameters of upper-sided geometric CUSUM charts.

p_0	p_1	k_H			h_H			
			In-Control ANIS†	300000	400000	500000	600000	700000 800000
0.00001	0.000015	81093		45886	62639	73081	80338	94102 106269
	0.000020	69315		31493	46783	56163	62599	67324 74086
	0.000030	54931		15072	28764	37009	42587	46636 49719
	0.000040	46210		5771	18595	26239	31371	35072 37876
			In-Control ANIS	60000	80000	100000	120000	160000 200000
0.00005	0.000075	16219		9178	12528	14617	16068	21255 25086
	0.000100	13863		6299	9357	11233	12520	14817 17995
	0.000150	10986		3014	5753	7402	8517	9943 10823
	0.000200	9242		1154	3719	5248	6274	7575 8371
			In-Control ANIS	30000	50000	70000	90000	110000 150000
0.0001	0.000150	8109		4588	7308	9409	11650	13339 16127
	0.000200	6931		3149	5616	6732	8267	9628 11573
	0.000300	5493		1507	3701	4663	5215	5751 7246
	0.000400	4621		577	2624	3507	4008	4332 4994
			In-Control ANIS	20000	30000	40000	50000	60000 70000
0.0002	0.000300	4055		3132	4017	5314	6272	7038 7723
	0.000400	3466		2340	3130	3705	4499	5095 5576
	0.000600	2746		1438	2129	2485	2705	3096 3465
	0.000800	2310		929	1568	1893	2092	2227 2358
			In-Control ANIS	15000	20000	25000	30000	40000 50000
0.0003	0.000450	2703		2279	2678	3349	3883	4691 5375
	0.000600	2310		1731	2086	2308	2755	3394 3856
	0.000900	1831		1111	1420	1609	1738	2065 2415
	0.001200	1540		761	1045	1218	1335	1484 1664
			In-Control ANIS	10000	15000	20000	25000	30000 35000
0.0004	0.000600	2027		1566	2008	2655	3134	3517 3859
	0.000800	1733		1170	1565	1852	2249	2547 2788
	0.001200	1373		719	1064	1243	1352	1548 1732
	0.001600	1155		465	784	947	1046	1113 1179
			In-Control ANIS	8000	12000	16000	20000	25000 30000
0.0005	0.000750	1622		1253	1607	2125	2509	2885 3226
	0.000100	1386		935	1252	1481	1798	2088 2314
	0.001500	1099		576	852	995	1083	1280 1450
	0.002000	924		372	627	757	837	901 998

†Due to the discrete nature of the geometric distribution, chart parameters are given such that the in-control ANIS is as close to the stated value as possible.

Table 4. The optimal chart parameters of upper-sided Bernoulli CUSUM charts.

p_0	p_1	c^*	h_S					
			In-Control ANIS[†]					
			300000	400000	500000	600000	700000	800000
0.00001	0.0000015	81093	1.1444	1.5658	1.7724	1.9012	1.9907	2.1604
	0.000020	69315	−	1.4543	1.6749	1.8102	1.9031	1.9713
	0.000030	54931	−	1.2744	1.5236	1.6737	1.7753	1.8490
	0.000040	46210	−	1.1249	1.4024	1.5678	1.6789	1.7589
			In-Control ANIS					
			60000	80000	100000	120000	160000	200000
0.00005	0.000075	16219	1.1494	1.5658	1.7724	1.9012	2.1604	2.4367
	0.000100	13863	−	1.4543	1.6749	1.8102	1.9712	2.1928
	0.000150	10986	−	1.2743	1.5236	1.6737	1.8489	1.9492
	0.000200	9242	−	1.1248	1.4023	1.5677	1.7588	1.8672
			In-Control ANIS					
			30000	50000	70000	90000	110000	150000
0.0001	0.000150	8109	1.1493	1.7724	1.9905	2.3103	2.5464	2.9165
	0.000200	6931	−	1.6748	1.9029	2.0685	2.2978	2.6084
	0.000300	5493	−	1.5234	1.7752	1.9050	1.9849	2.2622
	0.000400	4621	−	1.4023	1.6786	1.8195	1.9054	2.0210
			In-Control ANIS					
			20000	30000	40000	50000	60000	70000
0.0002	0.000300	4055	1.5657	1.9011	2.1603	2.4365	2.6449	2.8210
	0.000400	3466	1.4541	1.8099	1.9711	2.1927	2.3889	2.5421
	0.000600	2746	1.2739	1.6733	1.8485	1.9490	2.0462	2.1981
	0.000800	2310	1.1242	1.5671	1.7584	1.8667	1.9368	1.9861
			In-Control ANIS					
			15000	20000	25000	30000	40000	50000
0.0003	0.000450	2703	1.6826	1.9009	2.0725	2.3100	2.6445	2.9038
	0.000600	2310	1.5797	1.8095	1.9390	2.0680	2.3883	2.6078
	0.000900	1831	1.4167	1.6734	1.8143	1.9044	2.0464	2.2616
	0.001200	1540	1.2831	1.5669	1.7214	1.8188	1.9364	2.0201
			In-Control ANIS					
			10000	15000	20000	25000	30000	35000
0.0004	0.000600	2027	1.5654	1.9008	2.1593	2.4356	2.6443	2.8199
	0.000800	1733	1.4541	1.8096	1.9706	2.1922	2.3883	2.5418
	0.001200	1373	1.2739	1.6730	1.8478	1.9483	2.0459	2.1981
	0.001600	1155	1.1238	1.5671	1.7576	1.8667	1.9368	1.9853
			In-Control ANIS					
			8000	12000	16000	20000	25000	30000
0.0005	0.000750	1622	1.5654	1.9007	2.1597	2.4359	2.6905	2.9038
	0.000100	1386	1.4538	1.8095	1.9704	2.1919	2.4293	2.6075
	0.001500	1099	1.2739	1.6733	1.8480	1.9481	2.0883	2.2611
	0.002000	924	1.1234	1.5671	1.7576	1.8658	1.9502	2.0195

[*]k_S is obtained as $k_S = 1/c$.
[†]Due to the discrete nature of the Bernoulli distribution, chart parameters are given such that the in-control ANIS is as close to the stated value as possible.

Table 5. The optimal chart parameters of lower-sided Bernoulli CUSUM charts.

p_0	p_1	c^*				h_T		
			In-Control ANIS[†]	300000	400000	500000	600000	700000	800000
0.00001	0.000007	118892		1.1710	1.3762	1.5533	1.7100	1.8511	1.9802
	0.000005	138629		−	1.1654	1.3068	1.4308	1.5413	1.6412
	0.000003	171996		−	−	1.0420	1.1339	1.2154	1.2885
	0.000002	201180		−	−	−	−	1.0338	1.0933
			In-Control ANIS	60000	80000	100000	120000	160000	200000
0.00005	0.000035	23778		1.1710	1.3762	1.5533	1.7100	1.9801	2.2107
	0.000025	27726		−	1.1653	1.3068	1.4308	1.6412	1.8167
	0.000015	34399		−	−	1.0420	1.1339	1.2885	1.4158
	0.000010	40236		−	−	−	−	1.0932	1.1965
			In-Control ANIS	30000	50000	70000	90000	110000	150000
0.0001	0.000070	11889		1.1709	1.5533	1.8511	2.0994	2.3149	2.6789
	0.000050	13863		−	1.3068	1.5412	1.7324	1.8949	2.1635
	0.000030	17199		−	1.0420	1.2154	1.3550	1.4720	1.6618
	0.000020	20118		−	−	1.0337	1.1471	1.2419	1.3947
			In-Control ANIS	20000	30000	40000	50000	60000	70000
0.0002	0.000140	5945		1.3759	1.7097	1.9798	2.2103	2.4128	2.5941
	0.000100	6931		1.1653	1.4308	1.6412	1.8166	1.9681	2.1020
	0.000060	8600		−	1.1338	1.2884	1.4157	1.5241	1.6185
	0.000040	10059		−	−	1.0932	1.1963	1.2839	1.3601
			In-Control ANIS	15000	20000	25000	30000	40000	50000
0.0003	0.000210	3963		1.4676	1.7098	1.9167	2.0992	2.4128	2.6788
	0.000150	4621		1.2385	1.4306	1.5921	1.7323	1.9678	2.1634
	0.000090	5733		−	1.1338	1.2527	1.3548	1.5240	1.6616
	0.000060	6706		−	−	1.0641	1.1470	1.2839	1.3946
			In-Control ANIS	10000	15000	20000	25000	30000	35000
0.0004	0.000280	2927		1.3762	1.7100	1.9801	2.2106	2.4132	2.5945
	0.000200	3466		1.1650	1.4305	1.6408	1.8162	1.9677	2.1013
	0.000120	4300		−	1.1337	1.2881	1.4156	1.5240	1.6184
	0.000080	5029		−	−	1.0933	1.1965	1.2840	1.3601
			In-Control ANIS	8000	12000	16000	20000	25000	30000
0.0005	0.000350	2378		1.3755	1.7094	1.9794	2.2098	2.4596	2.6779
	0.000250	2773		1.1648	1.4302	1.6405	1.8161	2.0022	2.1626
	0.000150	3440		−	1.1337	1.2881	1.4154	1.5485	1.6613
	0.000100	4023		−	−	1.0932	1.1964	1.3040	1.3947

[*]k_T is obtained as $k_T = 1/c$.
[†]Due to the discrete nature of the Bernoulli distribution, chart parameters are given such that the in-control ANIS is as close to the stated value as possible.

6. Example of a High Yield Process

The wire bonding process in an integrated circuit (IC) assembly is a high yield process that provides an electrical connection between a semiconductor die and the external leads. The machine used for wire bonding is a highly advanced machine with a closed loop control system which is able to detect and rectify any deviation generated during the wire bonding process. With this highly capable and stable machine, nonconformities generated from this process are rare.

A two-sided Bernoulli CUSUM chart was used to monitor the wire bonding process. The upper-sided chart with parameters $k_S = 1/3466$ and $h_S = 2.1927$ and the lower-sided chart with parameters $k_T = 1/6931$ and $h_T = 1.8166$ are displayed in Figures 1 and 2 respectively. The upper-sided chart gives a "stepped" plot due to the fact that a nonconforming IC increases the CUSUM by $3465/3466$ while a conforming IC decreases the CUSUM by $1/3466$. The lower-sided chart also showed a "stepped" plot. Both the upper- and lower-sided charts found the process in statistical control.
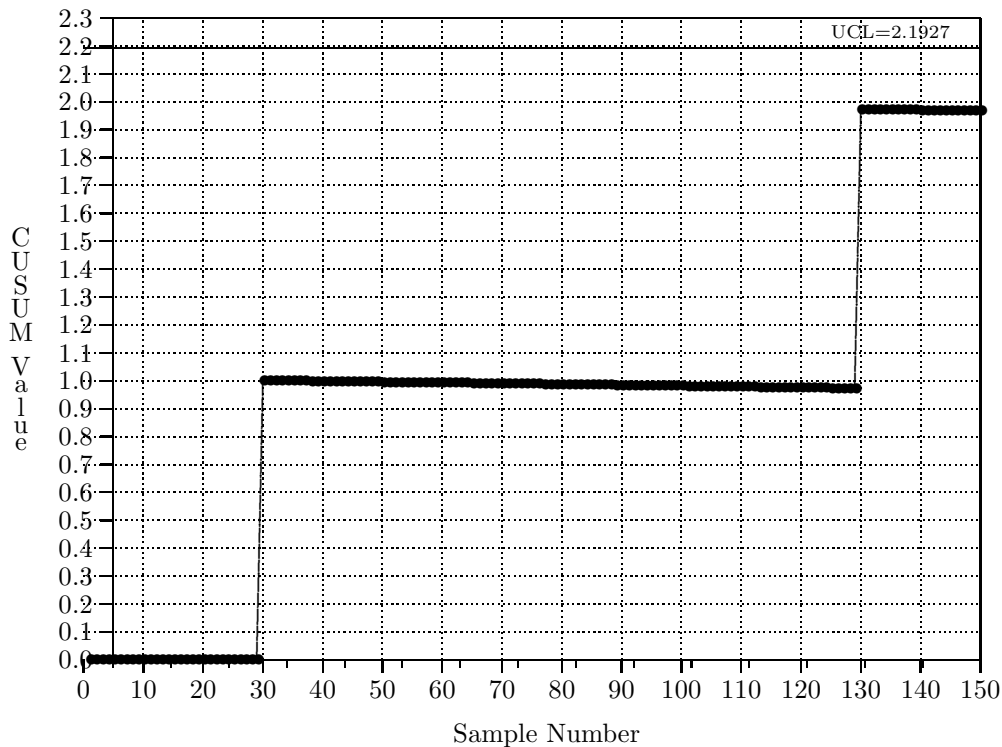
Figure 1. An upper-sided Bernoulli CUSUM chart for monitoring the fraction
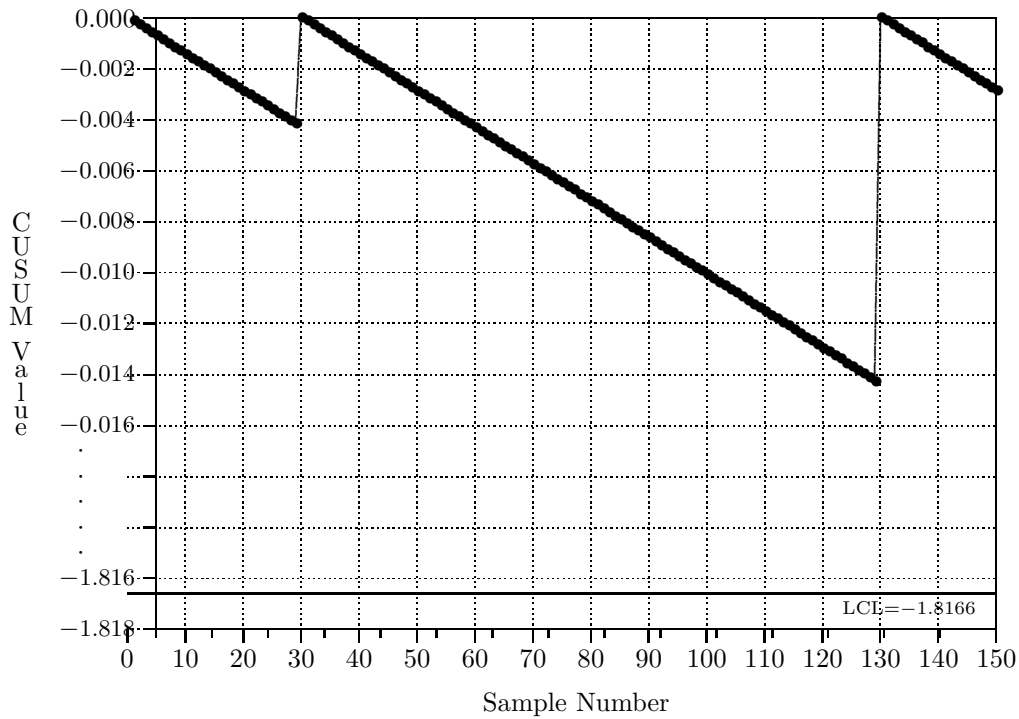of nonconforming integrated circuits produced.

Figure 2. A lower-sided Bernoulli CUSUM chart for monitoring the fraction of nonconforming integrated circuits produced.

Acknowledgements

Appendix

Equivalence between the bernoulli and geometric CUSUM charts

Denote the Bernoulli and geometric CUSUM charts by $B(k_S, h_S, u)$ and $G(k_H, h_H, w)$ respectively. We claim that $B(1/c, h, u(w))$ and $G(c, ch - c + 1, w)$ are equivalent for all w where $u(w) = (c + w - 1)/c$. To see this, first note that the upper-sided Bernoulli chart can issue a signal only when a nonconforming item is found.

Suppose that the first nonconforming item appears at the mth position. If $c + w - m \le 0$, then the values of $B(1/c, h, u(w))$ and $G(c, ch - c + 1, w)$ upon

inspecting the mth item are $(c-1)/c$ and 0, respectively. Viewing the mth position as the "origin", the two charts become $B(1/c, h, u(0))$ and $G(c, ch - c + 1, 0)$ with respective "head start" $u(0)$ and 0. If $c + w - m \geq ch - c + 1$, then both charts issue a signal upon inspecting the mth item. If $0 < c + w - m < ch - c + 1$, then the values of $B(1/c, h, u(w))$ and $G(c, ch - c + 1, w)$ at the mth item are $(c + (c + w - m) - 1)/c$ and $(c + w - m)$. Again, viewing the mth position as the "origin", the two charts become $B(1/c, h, u(c + w - m))$ and $G(c, ch - c + 1, c + w - m)$, respectively. We have shown that upon detecting the first nonconforming item, both charts either issue a signal or become two "new" charts with "head starts" u' and w' satisfying $u' = u(w')$. Thus the claim is proved.

ANIS of upper-sided Bernoulli CUSUM chart

The ANIS of an upper-sided CUSUM chart with parameters $k_S = 1/c$ and $h_S = (i + c)/c$ can be obtained using the Markov chain approach described by Brook and Evans (1972) and Page (1955). The matrix of in-control states $\mathbf{R}$ is given as

$$
\begin{array}{c c}
 & \begin{array}{ccccccccccc} 1 & 2 & \dots & i & i+1 & \dots & c & c+1 & \dots & c+i-1 & c+i \end{array} \\
\begin{array}{c} 1 \\ 2 \\ \vdots \\ i+1 \\ i+2 \\ \vdots \\ c+i \end{array} &
\left(\begin{array}{ccccccccccc}
q & 0 & \dots & 0 & 0 & \dots & p & 0 & \dots & 0 & 0 \\
q & 0 & \dots & 0 & 0 & \dots & 0 & p & \dots & 0 & 0 \\
\vdots & \ddots & \vdots & \vdots & \vdots & & \vdots & \vdots & \ddots & \vdots & \vdots \\
0 & 0 & \dots & q & 0 & \dots & 0 & 0 & \dots & 0 & p \\
0 & 0 & \dots & 0 & q & \dots & 0 & 0 & \dots & 0 & 0 \\
\vdots & \vdots & \vdots & \vdots & \vdots & \ddots & \vdots & \vdots & \vdots & \vdots & \vdots \\
0 & 0 & \dots & 0 & 0 & \dots & 0 & 0 & \dots & q & 0
\end{array}\right)
\end{array}
$$

where p is the fraction of nonconforming items and $q = 1 - p$. Let $\mu = (\mu_1, \dots, \mu_{i+c})$ be the vector of ANIS with μ_i be the ANIS with initial state i. Note that μ_1 is the ANIS with head start $u = 0$. The equations corresponding to $(\mathbf{I} - \mathbf{R})\mu = \mathbf{1}$ can be written as

$$
\begin{aligned}
\mu_1 &= 1 + q\mu_1 + p\mu_c, \\
\mu_j &= 1 + q\mu_{j-1} + p\mu_{c+j-1}, \quad j = 2, 3, \dots, i+1, \\
\mu_j &= 1 + q\mu_{j-1}, \quad j = i+2, i+3, \dots, i+c.
\end{aligned}
$$

Thus, μ_1 can be obtained recursively as

$$
\mu_1 = \frac{2\{1 - q^{c-1}(ip + 1)\} + q^{c-i-1}}{p(1 - q^{c-1} - ipq^{c-1})}, \quad \text{for } 0 \leq i \leq c-1,
$$

$$\mu_1 = a/b, \quad \text{for } c \leq i \leq 2c - 1,$$

where

$$a = q^{c-1} + 3q^{i-c+1} - 3q^i + pq^{c-1}\{(1+q^{c-1})(c-i-1)+(c-1)\}$$
$$+ \binom{i-c+2}{2} p^2 q^{c-2}(q^c - 3q^{i+1}) + 3pq^i\{q^{c-1}(i-c+1)(p(i-c+1)+1)-i\},$$

$$b = p^3 q^{i+c-1}\Big\{(c-i-1)^2 - \binom{i-c+2}{2}\Big\}$$
$$(c-i-1)p^2 q^i(1-q^{c-1}) + pq^i(q^{1-c} - p(c-1) - 1).$$

The ANIS with head start $u = (c-1)/c$ is given as $\mu_c = \mu_1 - 1/p$.

References

Bourke, P. D. (1991). Detecting a shift in the fraction of nonconforming items using run-length control charts with 100% inspection. *J. Qual. Tech.* **23**, 225-238.

Brook, D. and Evans, D. A. (1972). An approach to the probability distribution of CUSUM run length. *Biometrika* **59**, 539-549.

Calvin, T. W. (1987). Quality control techniques for 'zero-defects'. *IEEE Trans. Components, Hybrids and Manufacturing Technology* **6**, 323-328.

Goh, T. N. (1987). A control chart for very high yield processes. *Qual. Assur.* **13**, 18-22.

Lucas, J. M. (1985). Counted data CUSUM's. *Technometrics* **27**, 129-144.

McCool, J. I. and Motley, T. J. (1998). Control charts applicable when the fraction nonconforming is small. *J. Qual. Tech.* **30**, 240-247.

Moustakides, G. V. (1986). Optimal stopping times for detecting changes in distributions. *Ann. Statist.* **14**, 1379-1387.

Nelson, L. S. (1994). A control chart for parts-per-million nonconforming items. *J. Qual. Tech.* **26**, 239-240.

Page, E. S. (1955). Control charts with warning lines. *Biometrika* **42**, 243-257.

Quesenberry, C. P. (1995). Geometric Q charts for high quality processes (with discussion). *J. Qual. Tech.* **27**, 304-343.

Reynolds, M. R., Jr. and Stoumbos, Z. G. (1999). A CUSUM chart for monitoring a proportion when inspecting continuously. *J. Qual. Tech.* **31**, 87-108.

Siegmund, D. (1979). Corrected diffusion approximations in certain random walk problem. *Adv. Appl. Probab.* **11**, 701-719.

Siegmund, D. (1985). *Sequential Analysis.* Springer-Verlag, New York.

Infineon Technologies (Integrated Circuit), Sdn. Bhd., Melaka 75914, Malaysia.

E-mail: Tee-Chin.Chang@infineon.com

Department of Statistics and Applied Probability, National University of Singapore, Singapore 117543, Republic of Singapore.

E-mail: staganff@nus.edu.sg